

A NOVEL ADAPTIVE REMOTE SENSING PANSHARPENING ALGORITHM BASED ON THE ICM

H. T. Zhao^{1,2}, X. J. Li^{1,2,3*}, Y. K. Li^{1,2,3}, J. F. Ge^{1,2}, X. Y. Xu^{1,2}

¹Faculty of Geomatics, Lanzhou Jiaotong University, Lanzhou, China, xjli@mail.lzjtu.cn

²National-Local Joint Engineering Research Center of Technologies and Applications for National Geographic State Monitoring, Lanzhou, China

³Gansu Provincial Engineering Laboratory for National Geographic State Monitoring, Lanzhou, China

Commission III and IV

KEY WORDS: Pansharpening, Intersecting Cortical Model, Remote Sensing Image Fusion, Shuffled Frog Leaping Algorithm, Multispectral Image, Segmentation.

ABSTRACT:

In the paper, a novel Intersecting Cortical Network Model (ICM) based adaptive pansharpening algorithm is proposed to solve the deficiency of spectral distortion and texture detail missing in the remote sensing image fusion. The Shuffled Frog Leaping Algorithm (SFLA) is used in the proposed method to adaptively optimize the ICM model parameters. The fitness function of SFLA is constructed by fusion evaluation index Q4 and SAM, which can generate the irregular optimal segmentation regions. Then, these regions are used to adaptively extract the detail information of the panchromatic image. Finally, the sharpened higher resolution image is obtained with the weighted details and the multispectral upsampling image. Experiments are carried out with the WorldView-2 and GF-2 high-resolution datasets. The experimental results shown that the proposed algorithm performs better compared with the existing pansharpening fusion methods both in the spectral preservation and spatial detail enhancement, which verifies the effectiveness of the algorithm.

1. INTRODUCTION

Due to the limitation of the signal-to-noise ratio of remote sensing satellite sensors, it was difficult to obtain remote sensing images with both the high spatial resolution and the high spectral resolution. However, for the high precision applications, spectral information of the multispectral images (MS) and spatial information of the panchromatic images (PAN) need to be fused. Pansharpening is a commonly used remote sensing image fusion technology, which injects the spatial information of the PAN into the low-resolution MS images to acquire a fusion image with both high spatial and spectral resolutions (Yong et al., 2017). As an important part of the remote sensing image processing, pansharpening is of great significance for the subsequent interpretation, recognition and classification of remote sensing images (Li et al., 2019).

The pansharpening methods of the remote sensing images are mainly divided into three categories: multiresolution analysis (MRA) methods (Li et al., 2021), component substitution (CS) methods (Li et al., 2021) and sparse representation (SR) methods (Wang et al., 2011). The MRA methods extract the spatial details by using multiresolution analysis, and inject them into the MS images to improve the spatial resolution of the MS images. The MRA methods include Laplace pyramid decomposition (Alparone et al., 2008), wavelet transform (Vivone et al., 2020), nonsubsampling contourlet transform (Restaino et al., 2016). The CS methods transform the MS images into the transform domain, and then replace the spatial structure of the PAN images. Classical CS methods include intensity hue saturation (IHS) method (Bai et al., 2019), principal component analysis (PCA) (Li et al., 2021), gram schmidt (GS) transform methods (Alparone et al., 2007). Another pansharpening method is the SR method, which represents the image as a sparse signal with the

least coefficients in a complete space. Compared with the other traditional methods, SR method has higher robustness with the noise, but it is also time-consuming at the same time (Li et al., 2021). However, the traditional pansharpening methods take no account of the optimization of the fusion results, which will lead to the poor spectral preservation and spatial detail injection. The intersecting cortical model (ICM) is an improved single-layer neural network model based on pulse coupled neural network model (PCNN). Its unique biological background can enhance the details of the image, while retaining the contours of it. Therefore, the ICM model is beneficial for the pansharpening fusion tasks. However, the parameters of the ICM model is also determined and fixed by experience. Different parameters will result in the different fusion effects.

The paper proposes a novel pansharpening algorithm for remote sensing images. The proposed method takes advantages of the synchronization pulse segmentation characteristics of ICM and the global search ability of the Shuffled Frog Leaping Algorithm (SFLA), where the binary sub image information from the segmentation is used as details of the fusion result. The comparisons with the other classical fusion methods show that the proposed method not only achieves better spectral preservation, but also increases spatial texture details in the fusion result.

2. REMOTE SENSING IMAGE SEGMENTATION BASED ON ICM

2.1 ICM Network

Each neuron of ICM model is composed of input part, nonlinear pulse modulation part and pulse output part (Ma et al., 2006). The framework of a single ICM neuron model is shown in Figure 1.

*Corresponding author

When ICM model is applied to remote sensing image processing, a pixel represents a neuron (Pu et al, 2012). Its mathematical description is as follows:

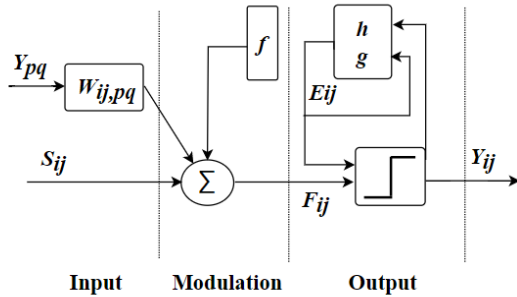


Figure 1. Neural model of ICM.

$$OP = \sum_{pq} W_{ijpq} \{Y_{pq}[n-1]\} \quad (1)$$

$$F_{ij}[n] = fF_{ij}[n-1] + S_{ij} + OP \quad (2)$$

$$Y_{ij}[n] = \begin{cases} 1 & \dots F_{ij}[n] > E_{ij}[n-1] \\ 0 & \dots \text{else} \end{cases} \quad (3)$$

$$E_{ij}[n] = gE_{ij}[n-1] + hY_{ij}[n] \quad (4)$$

Where S is the external activity stimulus. F represents the feedback input, and E denotes the dynamic activity threshold. f and g are the attenuation coefficients of F and E respectively. The coefficient h determines the increment of the threshold after the neuron is stimulated. The neuron of the ICM model is stimulated to generate the output pulses, when the feedback input F is greater than the dynamic threshold E . Then the threshold E greatly increases. After that, the threshold E continuously decreases with the attenuation factor g . The neuron will fire again, when the threshold E decreases until less than the feedback input F .

OP is the influenced by the neighbor neurons, which is composed of the pulse output Y_{pq} and weighting coefficient W_{ijpq} . In ICM iteration, neurons (i, j) will be affected by neighboring neurons (p, q) , causing the neuron to accelerate activation or inhibit activation. Y is the binary matrix output of ICM network, which can be used as the segmentation result of each iteration.

2.2 Image Segmentation with ICM

Each neuron of the ICM is connected to its neighboring neurons by W_{ijpq} , forming a single-layer 2D local connection network (Dai et al., 2015). The fired neurons will cause the synchronous release pulse of its neighboring neurons. Therefore, the output synchronous pulse sequence includes similar areas, edges, and texture information of the remote sensing images. The binary pulse sequences constitute the different segmentation images. In our proposed algorithm, the dynamic threshold is generally set to a large value to ensure each neuron will not be stimulated only once, thus ensure that each pixel belongs to a unique segmentation region (Li et al., 2019).

In Remote Sensing image fusion, the segmentation characteristic of ICM is mainly used. ICM divides the image into irregular regions, and the irregular statistical regions are easier to count the relevant pixel features with similar features and neighborhood relationships (Li et al., 2019). In ICM, different parameters will lead to different segmentation results.

3. ADAPTIVE REMOTE SENSING PANSHARPENING ALGORITHM BASED ON ICM

The paper proposes an ICM based adaptive remote sensing pansharpening algorithm. The step chart of the algorithm is shown in Figure 2. The proposed algorithm includes two main parts, ICM parameter adaptive design part, spatial detail extraction and injection part.

3.1 ICM Parameter Adaptive Design

In the paper, the SFLA is used to optimize the parameters of the ICM model to obtain the combined the optimal parameters f and g . SFLA imitates the process of the frog population distribution in the food searching, mainly includes two parts: local search and global information exchange (Zhang et al., 2018). The algorithm first performs a local search, and then uses the information sharing among subgroups to search for a global search. Here, we use it to find out the global optimal solution.

The method is to divide a frog population into several subgroups, and each frog only belongs to a specific subgroup (Zhang et al., 2018). Firstly, the fitness rules is set up to get the frog X_b with the best fitness, and the frog X_w with the worst fitness in the subgroup, and the best frog X_m among all frogs in the whole population. According to Eq. (5) and Eq. (7), the worst frog in the subgroup learns from the best frog, where D_j represents the leaping step size. The symbol $rand$ represents a random number between 0

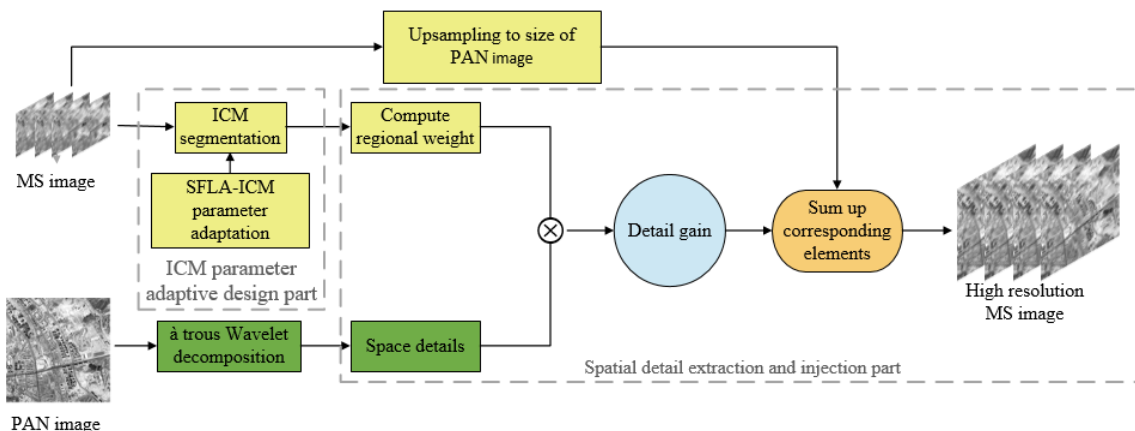


Figure 2. Schematic diagram of algorithm flow.

and 1 (Zhang et al., 2018). If the fitness value of the optimized frog X_{w1} is still lower than frog X_w in the atomic population, frog X_{w1} needs to be updated again through the global optimal method, as shown in Eq. (6) and Eq. (7).

$$D_j = rand * (X_b - X_w) \quad (5)$$

$$D_j = rand * (X_m - X_w) \quad (6)$$

$$X_{w1} = X_w + D_j \quad (7)$$

In our proposed method, each frog X is set as the ICM parameters f or g , and the process of searching for food means finding the optimal configuration of ICM parameters. The frogs in the population are divided into r subgroups. The quality evaluation ($Q4$) and the spectral angle mapping (SAM) are taken as the fitness function (Javan et al., 2021). With the optimization process of the parameters f and g in subgroups, its fitness is continuously improved. The value with higher fitness forms a new population, and then subdivides the new subgroup, until the fusion index achieves the optimal. The SFLA based ICM parameter optimization process is shown in Figure 3.

$$fitness = \frac{[Q4 + \cos(SAM)]}{2} \quad (8)$$

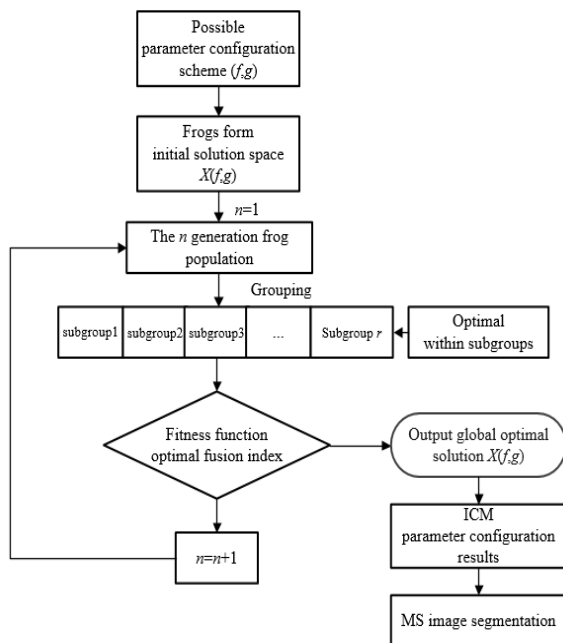


Figure 3. Process of ICM parameter optimization.

3.2 Spatial Detail Extraction and Injection

After the fusion parameter optimization of ICM, the iteration of adaptive ICM is used to segment the MS image by irregular clustering. On each clustering segmentation result, the detail injection weight is calculated by the standard deviation and covariance of the MS upsampling image, and so does the low spatial resolution PAN image. The larger injection weight means the greater correlation between the MS image and the PAN image in the clustering segmentation region. The implementation details of the fusion part are described as follows:

(1) Upsample the original multispectral image MS by the bicubic nonlinear interpolation to obtain MS_U with PAN size;

(2) Perform ‘à trous’ wavelet on panchromatic image, then decompose it into high-frequency and low-frequency images. Set high-frequency part to zero, and then perform inverse wavelet transform to obtain image P_L . The panchromatic image detail D_{PAN} is obtained according to Eq. (9) (Vivone et al., 2015), where PAN is the original panchromatic image;

(3) Segment the k -band multispectral images with adaptive parameter ICM. Calculate the gain weight w_k through Eq. (10) and Eq. (11). Where $Cov(A, B)$ stands for the covariance operation of A and B ; $Std(A)$ indicates the standard deviation of A ;

$$D_{PAN} = PAN - P_L \quad (9)$$

$$CR_k[n] = \begin{cases} \frac{Cov(MS_{U_k}(i,j), P_L(i,j))}{Cov(P_L(i,j), P_L(i,j))} if Y_{ij}[n] = 1 \\ 0 \end{cases} \quad (10)$$

$$w_k[n] = \begin{cases} \frac{Std(MS_{U_k}(i,j))}{Std(P_L(i,j))} if CR_k[n] > 0 \\ 0 \end{cases} \quad (11)$$

3.3 Fusion Rule

Calculate the fusion result I_{FU} by Eq. (12), the sharpened higher resolution image is obtained with the weighted details and the MS upsampling image.

$$I_{FU_k} = MS_U + w_k * D_{PAN}, k = 1, \dots, K \quad (12)$$

Where I_{FU_k} is the fusion image, MS_U is the upsampled MS image. D_{PAN} is the spatial detail of the PAN image. w_k is the gain weight. k represents each spectral channel of the multispectral images and K is the total number of spectral channels.

4 EXPERIMENTAL RESULTS

4.1 Experimental Datasets

The image datasets of the experiment are captured from the WorldView-2 and GF-2 remote sensing satellites. The first dataset represents the urban areas of Washington D.C. City with houses, roads, grassy areas and roads. The MS image of the dataset is characterized by four bands of blue, green, red and near-infrared with the space resolution 2m. And the space resolution of the PAN image is 0.5m. The second dataset is the suburban area of Lanzhou City, which consists of the mountainous. The space resolutions of the MS image and the PAN image are 4m and 1m respectively. The size of the MS images of all datasets are normalized to 512x512, and the size of the PAN images are cropped to 2048x2048.

4.2 Quality Assessment Criteria

Four quality evaluation indexes are used to objectively assess the proposed method, the $Q4$ index; the SAM index; the relative dimensionless global error in synthesis ($ERGAS$), and the spatial correlation coefficient (SCC) (Garzelli et al., 2009, Javan et al., 2021). The $Q4$ index takes into account both the spectral and the radiometric distortions; $ERGAS$ is a normalized index based on the root mean square error of the k th fused band to the reference; while SCC is used to evaluate the spatial correlation between the reference image and the fused image; and SAM measures only the

spectral distortion and measured in degrees; (Vivone et al., 2015, Vivone et al., 2020). The optimum value of $Q4$, $ERGAS$, SCC , and SAM are 1, 0, 1, 0, respectively.

4.3 Comparative Experiments

In order to examine the effectiveness of the proposed algorithm, six traditional pansharpening methods are prepared for comparison, such as GS method (Alparone et al., 2007), PCA

method (Li et al., 2021), Brovey method (Aiazzi et al., 2006), IHS method (Vivone et al., 2015), morphological operators based fusion method (MOF) (Restaino et al., 2016) and à trous wavelet decomposition method (ATWT) (Vivone et al., 2020). Figure 4(a) and Figure 5(a) are the original MS images of the datasets. Figure 4(b) and Figure 5(b) are the pansharpening results of our proposed method. Figure 4(c) ~ (h) and Figure 5(c) ~ (h) are the fusion results of the other comparison algorithm.

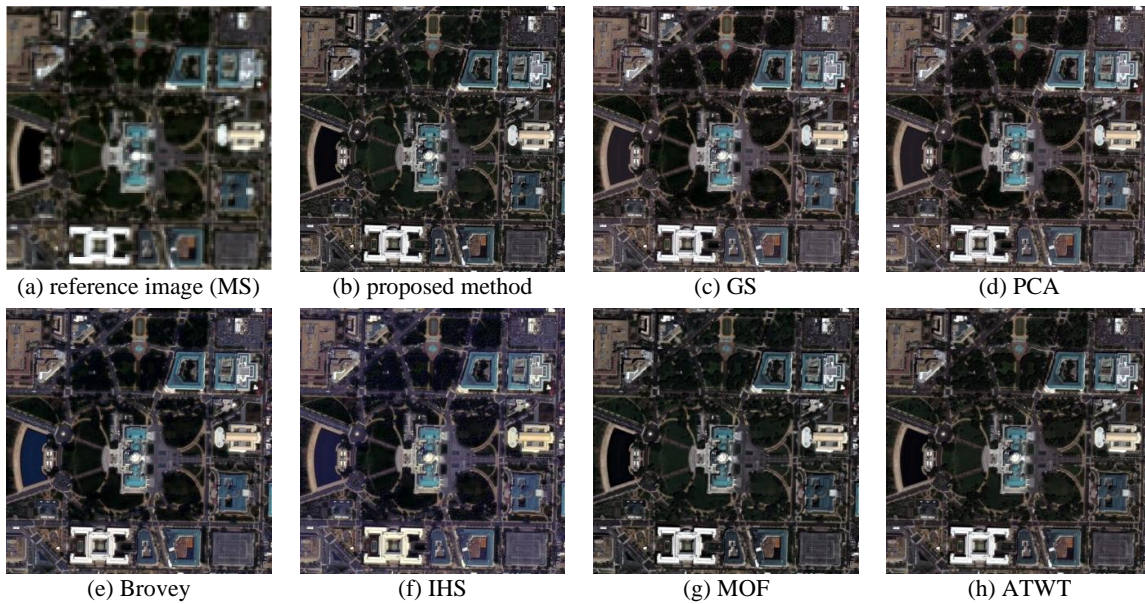


Figure 4. Comparison results of WorldView-2 dataset.

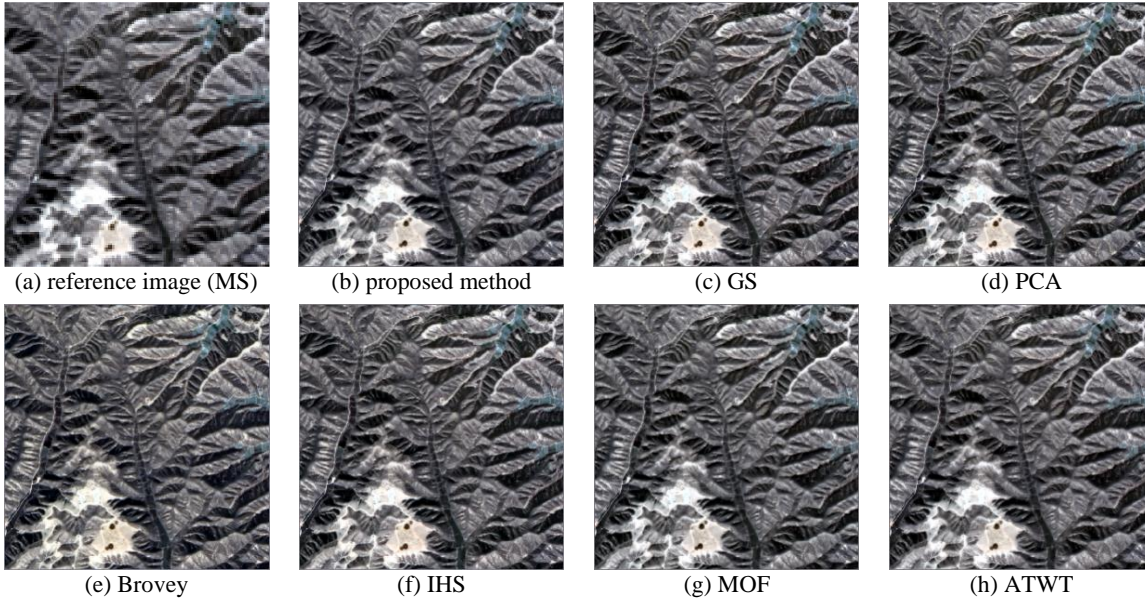


Figure 5. Comparison results of GF-2 dataset.

From Figures 4 and 5, it can be found that all the methods have improved the texture details of the original MS image. Figure 4(e) and Figure 5(e) show that Brovey method has large spectral distortions. The spectral distortion can also be seen in Figure 4(f). From Figures 5, we can see that all the methods can achieve an acceptable pansharpening fusion result. The green areas on the right side of the image are well preserved.

The quantitative index assessments are shown in Table 1 and Table 2. Obviously, among the four criteria of the image quality evaluation, the proposed method is superior to the other six methods in all criteria. It can be seen from Table 1 and Table 2 that the quality assessment criteria of the CS based methods are worse than those of the MRA based methods. This is due to the spectrum mismatch between the MS images transformation structure and the PAN images in the traditional CS method, during the process of transform the MS images into the transform

domain, and then replace the spatial structure of the PAN images. Furthermore, both the ATWT method and the proposed method extract the details of the PAN images based on the ‘à trous’ wavelet decomposition method, but the gain weight of the ATWT method is calculated through the whole image, while the

proposed method adaptively calculates the gain weight based on irregular regions. Therefore, the fusion image obtained by the proposed method has less spectral distortion and richer spatial texture information.

| Criterion | Proposed | GS | PCA | Brovey | IHS | MOF | ATWT |
|--------------|---------------|--------|--------|--------|--------|--------|--------|
| <i>Q4</i> | 0.8776 | 0.8212 | 0.8215 | 0.8177 | 0.8178 | 0.8670 | 0.8688 |
| <i>ERGAS</i> | 4.9428 | 5.7373 | 5.7268 | 5.8837 | 5.9094 | 5.2343 | 5.0097 |
| <i>SCC</i> | 0.7555 | 0.7549 | 0.7549 | 0.7475 | 0.7426 | 0.7495 | 0.7545 |
| <i>SAM</i> | 5.9615 | 6.5101 | 6.5057 | 6.4115 | 6.7940 | 6.3267 | 6.1609 |

Table 1. Quantitative comparative evaluation results of WorldView-2.

| Criterion | Proposed | GS | PCA | Brovey | IHS | MOF | ATWT |
|--------------|---------------|--------|--------|--------|--------|--------|--------|
| <i>Q4</i> | 0.9131 | 0.8405 | 0.8404 | 0.8325 | 0.8336 | 0.9035 | 0.9017 |
| <i>ERGAS</i> | 1.1845 | 1.6219 | 1.6229 | 1.5999 | 1.6332 | 1.3540 | 1.3033 |
| <i>SCC</i> | 0.8206 | 0.7578 | 0.7578 | 0.7561 | 0.7591 | 0.8015 | 0.7914 |
| <i>SAM</i> | 0.5633 | 0.6802 | 0.6809 | 0.6259 | 0.6953 | 0.6110 | 0.5795 |

Table 2. Quantitative comparative evaluation results of GF-2.

5 SUMMARY

In the paper, a novel adaptive ICM based pansharpening algorithm is proposed. First of all, the SFLA is used to adaptively optimize the segmentation results of ICM model parameters, which solves the problem of difficult selection of ICM parameters. Then, the irregular regions segmented by ICM are used for the image details extraction of PAN. Finally, the fusion result is obtained by the weighted details. The comparative experiments between WorldView-2 and GF-2 high-resolution datasets show that the proposed algorithm performs better in spatial details and spectral preservation of fusion results than other six methods. For the reason that, the ICM model conforms to the characteristics of the human vision system, and the SFLA is used to further improve the fusion accuracy, the proposed method presents the less spectral distortion and better spatial texture details. Another advantage of the proposed method is that all the parameters of ICM model are acquired adaptively rather than set by experience in the traditional ICM. Furthermore, determining the strategy of the parameter configuration adaptively by the other advanced algorithms such as deep learning optimization algorithms is our future work.

ACKNOWLEDGEMENTS

This paper is jointly supported by National Natural Science Foundation of China (No. 41861055), China Postdoctoral Science Foundation (No. 2019M653795) and lzjtu EP Program (No. 201806).

REFERENCES

Aiazzi, B., Alparone, L., Baronti, S., et al., 2006. MTF-tailored multiscale fusion of high-resolution MS and Pan imagery. *Photogrammetric Engineering & Remote Sensing*, 72(5), 591-596.

Alparone, L., Aiazzi, B., Baronti, S., et al., 2008. Multispectral and panchromatic data fusion assessment without reference. *Photogrammetric Engineering & Remote Sensing*, 74(2), 193-200.

Alparone, L., Wald, L., Chanussot, J., et al., 2007. Comparison of Pansharpening Algorithms: Outcome of the 2006 GRS-S Data Fusion Contest. *IEEE Transactions on Geoscience and Remote Sensing*, 45(10), 3012-3021.

Bai, X., Wei, L., 2019. Remote sensing image fusion algorithm based on IHS transform coupled with adaptive regional features. *Journal of Electronic Measurement and Instrumentation*, 33(2), 161-167.

Dai, W. Z., Hu, W. S., 2016. Medical image fusion algorithm based on improved intersecting cortical model. *Application Research of Computers*, 33(9), 2852-2855.

Garzelli, A., Nencini, F., 2009. Hypercomplex quality assessment of multi/hyperspectral images. *IEEE Geoscience and Remote Sensing Letters*, 6(4), 662-665.

Javan, F. D., Samadzadegan, F., Mehravar, S., et al., 2021. A review of image fusion techniques for pansharpening of high-resolution satellite imagery. *ISPRS Journal of Photogrammetry and Remote Sensing*, 171, 101-117.

Li, S. T., Li, C. Y., Kang, X. D., 2021. Development status and future prospects of multi-source remote sensing image fusion. *National Remote Sensing Bulletin*, 25(1), 148-166.

Li, X. J., Yan, H. W., Yang, S. W., et al., 2019. A fusion algorithm of multispectral remote sensing image and aerial image. *Remote Sensing Information*, 34(4), 11-15.

Ma, Y. D., Qi, C. L., 2006. Study of Automated PCNN System Based on Genetic Algorithm. *Journal of System Simulation*, 18(3), 722-725.

Pu, T., Li, Y. H., Cheng, J., et al., 2012. Color image enhancement based on improved intersecting cortical model. *Journal of Computer Applications*, 32(11), 3153-3156.

Restaino, R., Vivone, G., Mura, M. D., et al., 2016. Fusion of multispectral and panchromatic images based on morphological operators. *IEEE Transactions on Image Processing*, 25(6), 2882-2895.

- Vivone, G., Alparone, L., Chanussot, J., et al., 2015. A critical comparison among pansharpening algorithms. *Transactions on Geoscience and Remote Sensing*, 53(5), 2565-2586.
- Vivone, G., Stefano, M., Jocelyn, C., 2020. Pansharpening: Context-based generalized Laplacian pyramids by robust regression. *Transactions on Geoscience and Remote Sensing*, 58(9), 6152-6167.
- Wang, X. Y., Liu, Y, Jiang, Z. Y., 2011. An IHS Fusion Method based on Structural Similarity. *Remote Sensing Technology and Application*, 26(5), 670-676.
- Yong, Y., Wan, W., Huang, S., et al., 2017. A novel pan-Sharpening framework based on Matting Model and Multiscale Transform. *Remote Sensing*, 9(4), 391.
- Zhang, X. M., Cheng, J. F., Kang, Q., et al., 2018. Improved Shuffled Frog Leaping Algorithm and its application in multi threshold image segmentation. *Computer Science*, 45(8), 54-62.